Supplemental Information

Table S1: Differentially regulated pathways in cortical versus cerebellar human astrocytes following treatment with PBS or IFN-β

Pathway	p value
Regulation of eIF4 and p70S6K signaling	3.64E-07
EIF2 signaling	4.10E-07
Chondroitin and dermatan biosynthesis	7.23E-05
Interferon signaling	**1.12E-04**
Mevalonate pathway	1.95E-04
Tight junction signaling	**2.18E-04**
Geranylgeranyldiphosphate biosnthesis	4.51E-04
Epithelial adherens junction signaling	**5.38E-04**
IRF activation by cytosolic PRRs	**9.20E-04**
EIF2 signaling	1.01E-03
Aryl hydrocarbon receptor signaling	1.43E-03
HMGB1 signaling	1.50E-03
Retinoic acid-mediated apoptosis	**1.50E-03**
AMPK signaling	1.70E-03
Cardiovascular hypoxia	1.80E-03
Cholesterol biosynethesis	2.02E-03
mTOR signaling	2.28E-03
Actin cytoskeleton signaling	2.30E-03
Retinoate biosynthesis	2.60E-03
Vitamin-C transport	3.42E-03
Granulocyte adhesion and diapedesis	4.20E-03
Neuronal nNOS signaling	4.29E-03
Death receptor signaling	**4.81E-03**
Chondroitin sulfate biosynthesis	5.34E-03
Nicotine degradation	6.45E-03
Calpain protease regulation	7.35E-03

Table S2: Selected genes differentially expressed between regions in PBS treated astrocyte cultures

Genes upregulated in CBL astrocytes vs. CTX astrocytes following PBS treatment

Rank	Gene symbol	Fold change (CBL vs. CTX)
1	TGM2	5.519
2	HAPLN1	5.363
3	CFH	5.295
4	PADI2	5.272
5	CORIN	4.936
6	SLC38A2	4.745
7	ATXN1	4.591
8	EDIL3	4.407
9	TREX1	4.297
10	FGF14	4.114
11	SEMA3C	3.965
12	SDC4	3.883
13	C10orf41	3.878
14	TSIX	3.846
15	WNT5A	3.792
16	OPA3	3.766
17	HPS3	3.731
18	KRT18	3.668
19	TNRC6C	3.505
20	C1orf170	3.422
21	NR2F2	3.409
22	C7orf49	3.365
23	CYP1B1	3.265
24	COL12A1	3.248
25	C1orf204	3.242
26	ALDH1A3	3.214
27	UNC84B	3.149
28	LMO7	3.079
29	ITGBL1	3.068
30	VAMP1	2.999
31	IFIT3	2.969
32	CSNK1D	2.933
33	CLDN11	2.888
34	FLJ30064	2.805
35	EMILIN1	2.803
36	MTERFD2	2.789
37	SMG6	2.772
38	RBM9	2.758

Genes downregulated in CBL astrocytes vs. CTX astrocytes following PBS treatment

Rank	Gene symbol	Fold change (CBL vs. CTX)
1	HEPN1	-7.493
2	BSCL2	-6.881
3	IDH3A	-5.951
4	PTPRZ1	-5.921
5	NCAN	-5.857
6	HOPX	-5.846
7	FABP7	-5.831
8	KIF5C	-5.597
9	GLB1L2	-5.084
10	CELSR2	-5.063
11	GAP43	-4.953
12	TCFL5	-4.806
13	CXCR6	-4.321
14	HLA-DQA1	-4.222
15	PVRIG	-4.184
16	DENND1A	-4.163
17	NUBP1	-4.121
18	FAM13C	-3.777
19	TNKS	-3.662
20	SYT11	-3.502
21	FILIP1	-3.355
22	PMP22	-3.255
23	CA14	-3.247
24	YIF1A	-3.148
25	TUBB2B	-3.146
26	SOX2	-3.082
27	FZD8	-3.047
28	MTG1	-2.935
29	IVNS1ABP	-2.913
30	PDE6B	-2.912
31	PEG3AS	-2.877
32	HMGCS1	-2.851
33	C17orf45	-2.811
34	CADM1	-2.769
35	HMGCR	-2.756
36	SLC15A1	-2.724
37	C8orf59	-2.687
38	CD27	-2.611

39	HDAC9	2.672
40	DNAJB4	2.615
41	PLOD2	2.558
42	MGST1	2.525
43	GDF5OS	2.505
44	ZFHX4	2.49
45	SP100	2.471
46	MEST	2.418
47	PLEKHG6	2.387
48	PDE4DIP	2.343
49	TOR1A	2.332
50	COL6A2	2.321
51	PIP4K2B	2.295
52	RPL13A	2.288
53	PARP14	2.27
54	CSGALNACT1	2.255
55	SBF2	2.23
56	NT5C1B	2.199
57	PAFAH1B1	2.195
58	FSTL3	2.177
59	P4HA1	2.17
60	DUSP6	2.159
61	TRAM1	2.152
62	ANKRD40	2.117
63	EFEMP1	2.102
64	FAM3C	2.099
65	IL1R1	2.094
66	MX1	2.039
67	TGFBR1	2.035
68	USO1	2.026
69	IRS1	2.024
70	GBP1	1.965
71	ALCAM	1.93
72	PLXNA4	1.918
73	APOL2	1.895
74	ADAM12	1.887
75	LAMA2	1.874
76	DDX58	1.847
77	SYNPO	1.832
78	FNDC8	1.802
79	PGK1	1.797
80	EPHX1	1.796
81	BCAT1	1.787
82	SAMHD1	1.699

39	JAG1	-2.506
40	IQCK	-2.476
41	NES	-2.447
42	SLC15A3	-2.427
43	ANKRD42	-2.408
44	CTSB	-2.365
45	JMJD4	-2.36
46	SLC25A26	-2.321
47	FOXG1	-2.247
48	STK11	-2.186
49	RPL23AP64	-2.172
50	GEMIN7	-2.166
51	TUBB1	-2.166
52	ZWILCH	-2.159
53	RAB41	-2.085
54	THBS3	-2.048
55	PDE8B	-2.042
56	NNT	-2.035
57	PAPPA	-2.032
58	ABR	-2.021
59	IER3	-2.017
60	CTGF	-2.003
61	SIRT5	-2.003
62	NCAM1	-1.962
63	KIAA0182	-1.958
64	HADHA	-1.903
65	TIAM2	-1.897
66	FLNC	-1.89
67	CBL	-1.873
68	SYNM	-1.867
69	TOP2A	-1.818
70	CDH2	-1.808
71	ARSB	-1.803
72	CCNI2	-1.796
73	TMEM91	-1.787
74	RRS1	-1.76
75	PAX6	-1.759
76	SMARCA4	-1.732
77	C15orf37	-1.73
78	NUDT13	-1.729
79	VPS13B	-1.702
80	OGFOD1	-1.696
81	LMOD1	-1.672
82	DDB2	-1.671

83	MYL12A	1.695
84	SEC23A	1.682
85	DTX3L	1.524
86	LRP1	1.523
87	PPIB	1.523
88	DCBLD2	1.476
89	FANCL	1.46
90	TJP1	1.429
91	UBAC2	1.4
92	HEATR1	1.397
93	IFI16	1.385
94	CAPN2	1.35
95	PPP3CA	1.336
96	EIF3B	1.276
97	IFIH1	1.258
98	IFI44L	1.083
99	IFIT1	0.721
100	STAT1	0.572

83	PUS10	-1.65
84	PEX1	-1.644
85	PEG10	-1.639
86	IDI1	-1.624
87	MRPS7	-1.618
88	TRAPPC2	-1.604
89	MARCKSL1	-1.604
90	PTGR2	-1.601
91	DOM3Z	-1.591
92	CLU	-1.587
93	FAM169A	-1.581
94	UBE2H	-1.572
95	LIMK2	-1.569
96	HMGB2	-1.553
97	LPIN3	-1.528
98	DDR1	-1.511
99	ASAP2	-1.487
100	PCCA	-1.482

Table S3: Selected genes differentially expressed between regions in IFN-β treated astrocyte cultures

Genes upregulated in CBL astrocytes vs. CTX astrocytes following IFN-β treatment

Rank	Gene symbol	Fold change (CBL vs. CTX)
1	CFH	6.894
2	PADI2	6.051
3	HPS3	5.11
4	IL1R1	4.721
5	HAPLN1	4.599
6	CLDN11	4.578
7	CSGALNACT1	4.311
8	ITGBL1	4.272
9	TSIX	4.172
10	CORIN	4.139
11	GBP1	4.111
12	FGF14	3.844
13	ALCAM	3.833
14	C1orf170	3.821
15	CDH11	3.784
16	FAM151A	3.746
17	CSNK1D	3.651
18	GLIS2	3.623
19	TREX1	3.596
20	VAMP1	3.503
21	FEM1B	3.478
22	EDIL3	3.333
23	FLJ30064	3.309
24	PDE4DIP	3.231
25	UACA	3.224
26	IGFBP4	3.179
27	SLC38A2	3.136
28	CCDC152	3.135
29	TGM2	3.128
30	CYP1B1	3.012
31	NRP1	2.999
32	CSRP1	2.895
33	KRT18	2.886
34	DNAJB4	2.857
35	CCDC80	2.823
36	OPA3	2.795
37	LAMA2	2.79
38	ERRFI1	2.777

Genes downregulated in CBL astrocytes vs. CTX astrocytes following IFN-β treatment

Rank	Gene symbol	Fold change (CBL vs. CTX)
100	HEPN1	-8.102
99	NCAN	-7.955
98	PTPRZ1	-6.808
97	MKRN3	-6.633
96	FABP7	-6.077
95	HOPX	-5.935
94	CXCR6	-5.575
93	BSCL2	-4.817
92	PDE6B	-4.68
91	NUBP1	-4.629
90	GAP43	-4.607
89	ARSB	-4.576
88	SYT11	-4.544
87	JAG1	-4.437
86	TNKS	-4.434
85	KIAA0746	-4.388
84	KIF5C	-4.228
83	SLC1A3	-4.225
82	FAM13C	-4.207
81	IDH3A	-3.792
80	TUBB2B	-3.735
79	SMAP1	-3.648
78	FZD8	-3.629
77	PHYHIPL	-3.504
76	CADM1	-3.231
75	PMP22	-3.155
74	ISLR	-3.129
73	SMC5	-3.106
72	NAV2	-3.063
71	DENND1A	-3.042
70	PVRIG	-3.022
69	GLB1L2	-2.972
68	CELSR2	-2.921
66	THBS3	-2.765
67	BAZ2B	-2.765
65	SYNM	-2.752
64	YIF1A	-2.748
63	CASP6	-2.709

39	COL12A1	2.757
40	ADAMTS1	2.717
41	COL8A1	2.7
42	NR2F2	2.695
43	PLS3	2.694
44	C1orf138	2.694
45	TMEM39A	2.663
46	NT5C1B	2.658
47	HOXB3	2.637
48	FKBP5	2.55
49	MTERFD2	2.539
50	SPAG4	2.536
51	COL6A3	2.526
52	ODZ2	2.477
53	CALHM2	2.475
54	TFPI	2.45
55	WNT5A	2.423
56	CAV1	2.412
57	TNRC6C	2.411
58	EPB41	2.399
59	LMO7	2.398
60	ZNF687	2.385
61	RGS4	2.362
62	NOTCH2	2.359
63	MBNL1	2.359
64	NOTCH2	2.359
65	EIF3B	2.354
66	DDX58	2.34
67	FNDC8	2.328
68	COL6A1	2.323
69	PLP2	2.295
70	SDC4	2.293
71	IRS1	2.285
72	LTBP1	2.284
73	PPP2R1B	2.277
74	TXNIP	2.256
75	CSGALNACT2	2.256
76	TXNIP	2.256
77	RPS4X	2.248
78	PRPF40B	2.239
79	SFRS3	2.232
80	GDF5OS	2.222
81	AP3M1	2.222
82	GDF5OS	2.222

62	PEG3AS	-2.708
61	PEG10	-2.638
60	HMGCS1	-2.627
59	TCFL5	-2.59
58	SLC15A3	-2.535
57	NMT1	-2.497
56	C17orf45	-2.485
55	CTTNBP2NL	-2.469
54	IPO4	-2.468
53	RAB41	-2.442
52	MTG1	-2.439
51	PKLR	-2.42
50	IVNS1ABP	-2.392
49	FADS1	-2.379
48	PTN	-2.376
47	HLA-DQA1	-2.366
46	DDB2	-2.354
45	CLCN3	-2.352
44	SLC5A10	-2.28
43	C22orf15	-2.267
42	SOX11	-2.257
41	SORT1	-2.256
40	PCCA	-2.252
39	SOX2	-2.222
38	CCNI2	-2.219
37	DDR1	-2.214
36	SIRT5	-2.131
35	FILIP1	-2.065
34	CCL2	-2.063
33	PAX6	-2.061
32	HADHA	-2.032
31	RAB31	-1.989
30	ITGA3	-1.976
29	C8orf59	-1.928
28	HMGCR	-1.922
27	SMTNL1	-1.916
26	DLEC1	-1.852
25	NAP1L4	-1.85
24	NRP2	-1.843
23	TOP2A	-1.83
22	JMJD4	-1.818
21	SEMA6A	-1.816
20	SLC25A19	-1.813
19	PPP1CB	-1.811

83	GNG3	2.216
84	SAFB	2.21
85	DZIP1	2.197
86	ALDH1A3	2.184
87	SEC23A	2.168
88	RAB23	2.163
89	PLXNA4	2.155
90	EMILIN1	2.128
91	CLDN22	1.447
92	IFIH1	1.41
93	TJP1	1.363
94	IFIT2	0.636
95	IFIT3	0.557
96	STAT1	0.379
97	MX1	0.249
98	RSAD2	0.249
99	IFIT1	0.249
100	IFI44L	0.249

18	ACAD11	-1.799
17	NOX1	-1.79
15	TRAPPC2	-1.789
16	ECHDC1	-1.789
14	ZNF45	-1.788
13	FLJ35848	-1.755
12	CTSB	-1.751
11	FOXG1	-1.741
10	MYBBP1A	-1.737
9	SCD	-1.72
7	ZWILCH	-1.718
8	VPS13B	-1.718
6	STK11	-1.717
5	RNF220	-1.716
4	GEMIN7	-1.689
3	NDFIP1	-1.679
2	BID	-1.678
1	CA14	-1.627

Table S4: Primary sequences for qRT-PCR studies

Target	Species	Direction 5' – 3'	Sequence
CXCL11	Human	Forward	GCTATAGCCTTGGCTGTGATAT
		Reverse	GCCTTGCTTGCTTCGATTTGGG
GAPDH	Human	Forward	GAAGGTGAAGGTCGGAGTC
		Reverse	GAAGATGGTGATGGGATTTC
IFIT1	Human	Forward	GAAGGTGAAGGTCGGAGTC
		Reverse	GGCTGATATCTGGGTGCCTA
IFN-α	Human	Forward	GGTGCTCAGCTGCAAGTCAA
		Reverse	GCTACCCAGGCTGTGGGTT
IRF3	Human	Forward	ACCAGCCGTGGACCAAGAG
		Reverse	TACCAAGGCCCTGAGGCAC
IRF7	Human	Forward	TGGTCCTGGTGAAGCTGGAA
		Reverse	GATGTCGTCATAGAGGCTGTTGG
OAS1	Human	Forward	CAAGCTCAAGAGCCTCATCC
		Reverse	TGGGCTGTGTTGAAATGTGT
TLR3	Human	Forward	TCCCAAGCCTTCAACGACTG
		Reverse	TGGTGAAGGAGAGCTATCCACA
TLR7	Human	Forward	TTACCTGGATGGAAACCAGCTAC
		Reverse	TCAAGGCTGAGAAGCTGTAAGCTA
VCAM	Human	Forward	TTTGGGAACGAACACTCTTACC
		Reverse	CTTGACTGTGATCGGCTTCC
CCL2	Mouse	Forward	TGGCTCAGCCAGATGCAGT
		Reverse	TTGGGATCATCTTGCTGGTG
CXCL10	Mouse	Forward	GCCGTCATTTTCTGCCTCA
		Reverse	CGTCCTTGCGAGAGGGATC
GAPDH	Mouse	Forward	GGCAAATTCAACGGCACAGT
		Reverse	AGATGGTGATGGGCTTCCC
IFIT1	Mouse	Forward	CTGAGATGTCACTTCACATGGAA
		Reverse	GTGCATCCCCAATGGGTTCT
IFN-α	Mouse	Forward	CTTCCACAGGATCACTGTGTACCT
		Reverse	TTCTGCTCTGACCACCTCCC
IFN-β	Mouse	Forward	CTGGAGCAGCTGAATGGAAAG
		Reverse	CTTCTCCGTCATCTCCATAGGG
IL-1β	Mouse	Forward	ACCTGTCCTGTGTAATGAAAGACG
		Reverse	TGGGTATTGCTTGGGATCCA
OAS1	Mouse	Forward	GGGCCTCTAAAGGGGTCAAG
		Reverse	TCAAACTTCACTCCACAACGTC
TLR3	Mouse	Forward	CTCTTGAACAACGCCCAACT
		Reverse	GTCCACTTCAGCCCAGAGAA
TLR7	Mouse	Forward	ACAGAAATCCCTGAGGGCATT
		Reverse	CAGATGGTTCAGCCTACGGAAG
TNF-α	Mouse	Forward	GCACAGAAAGCATGATCCG
		Reverse	GCCCCCCATCTTTTGGG
VCAM	Mouse	Forward	CAAATCCTTGATACTGCTCAT
		Reverse	TTGACTTCTTGCTCACAGC
Viperin	Mouse	Forward	TGCTGGCTGAGAATAGCATTAGG
		Reverse	GCTGAGTGCTGTTCCCATCT

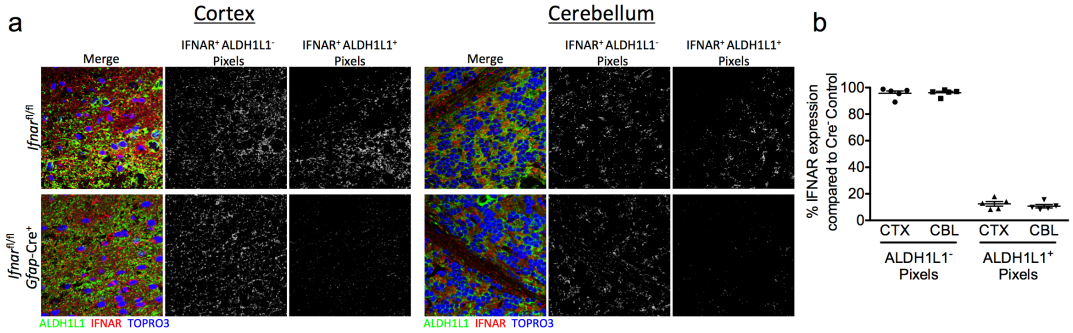

Figure S1: IFNAR deletion in astrocytes of *Ifnar*$^{fl/fl}$ *Gfap*-Cre^{+} mice. (**a**) IHC detection of astrocyte marker ALDH1L1 (green) and IFNAR (red) in the cerebral cortex and cerebellum of uninfected *Ifnar*$^{fl/fl}$ and *Ifnar*$^{fl/fl}$ *Gfap*-Cre^{+} mice. Nuclei are shown in blue. Colocalized signal is shown in white. Images are representative of at least 4 images taken for each of 5 independent mice per genotype. (**b**) Quantification of colocalized signal of images represented in (**a**). Values are reported as percent of double positive pixels in Cre^{+} mice compared to mean values for Cre^{-} mice. Values in (**b**) are derived from 5 independent mice per genotype.

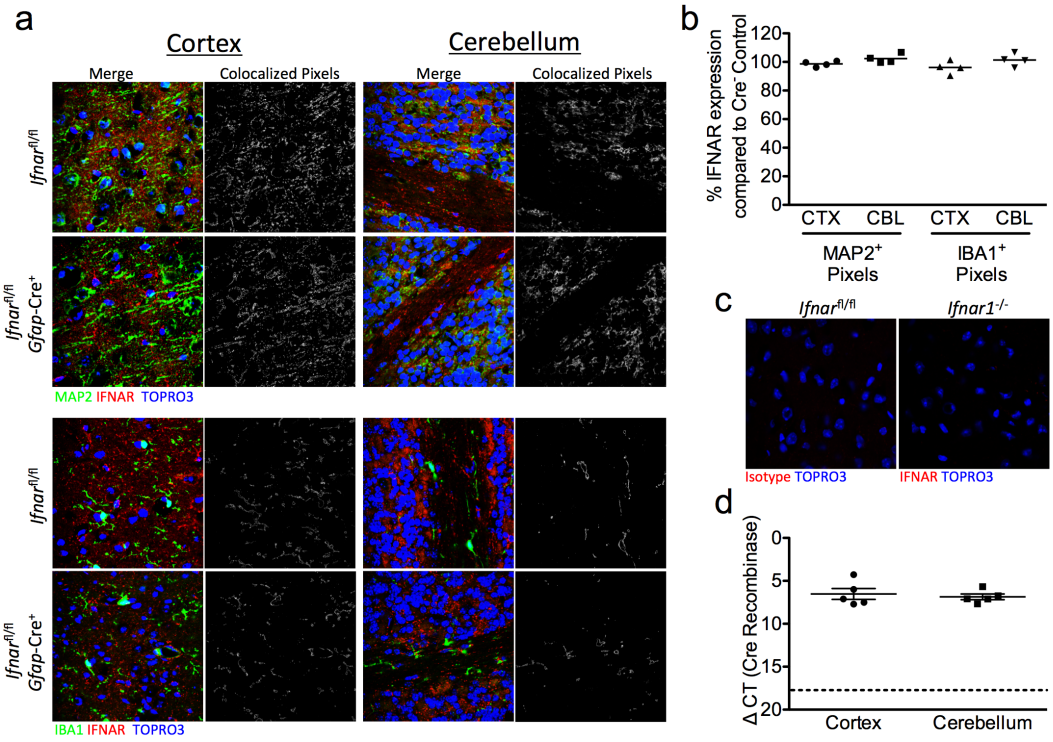

Figure S2: IFNAR expression in neurons and microglia of *Ifnar*$^{fl/fl}$ *Gfap*-Cre^{+} mice. (**a)** IHC detection of neuron marker MAP2 or microglial marker IBA-1 (green) and IFNAR (red) in the cerebral cortex and cerebellum of naïve *Ifnar*$^{fl/fl}$ and *Ifnar*$^{fl/fl}$ *Gfap*-Cre^{+} mice. Nuclei are shown in blue. Colocalized signal is shown in white. Images are representative of at least 4 images taken for each of 4 independent mice per genotype. (**b**) Quantification of colocalized signal of images represented in (**a**). Values are reported as percent of double positive pixels in Cre^{+} mice compared to mean values for Cre^{-} mice. (**c)** Control stains using a matched IgG isotype antibody in *Ifnar*$^{fl/fl}$ (left) or IFNAR antibody in *Ifnar1*$^{-/-}$ tissue sections from the cerebral cortex (right). (**d**) qRT-PCR analysis of Cre recombinase expression in cerebral cortex and cerebellum of *Ifnar*$^{fl/fl}$ *Gfap*-Cre^{+} mice. Cycle threshold (Ct) values were normalized to Ct values of the housekeeping gene GAPDH. Values in (**b**) and (**d**) are derived from 4 or 5 independent mice per genotype, respectively.

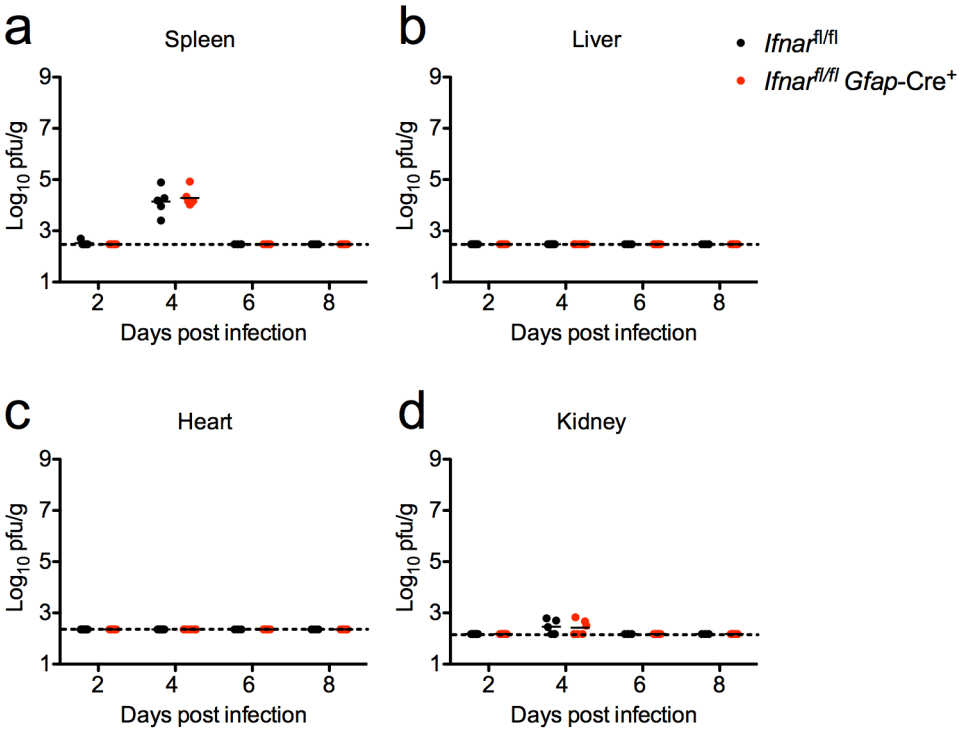

Figure S3: Peripheral organ titers following subcutaneous inoculation. Mice in (**a-d**) were infected subcutaneously with WNV (New York 2000). Peripheral organs were harvested on indicated days and assessed for viral burden by standard plaque assay. All values collected from 4-6 mice per group, and were pooled from two independent experiments. All data were compared via Mann-Whitney test.

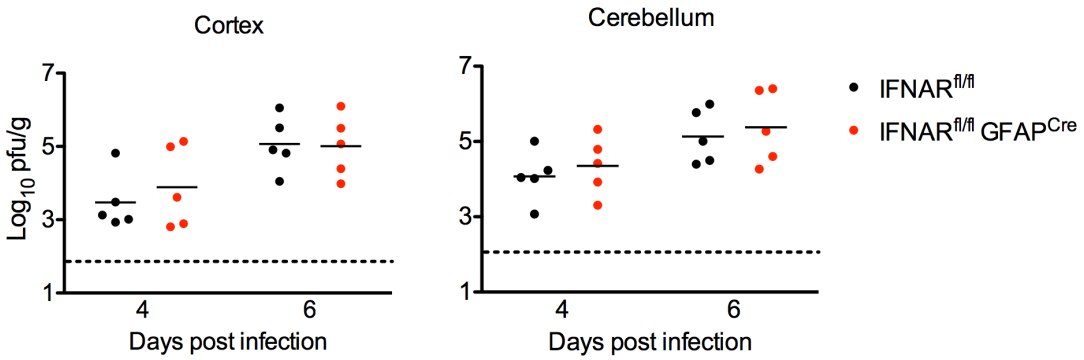

Figure S4: CNS titers following intracerebellar inoculation with WNV-Madagascar. Mice were inoculated via intracerebellar route with 10^4 PFU of WNV-Madagascar and CNS regions were harvested on indicated days following infection. Brain regions were assayed for viral burden by standard plaque assay. Data are pooled from two independent experiments with a total of 5 mice per group. All data were compared via Mann-Whitney test.

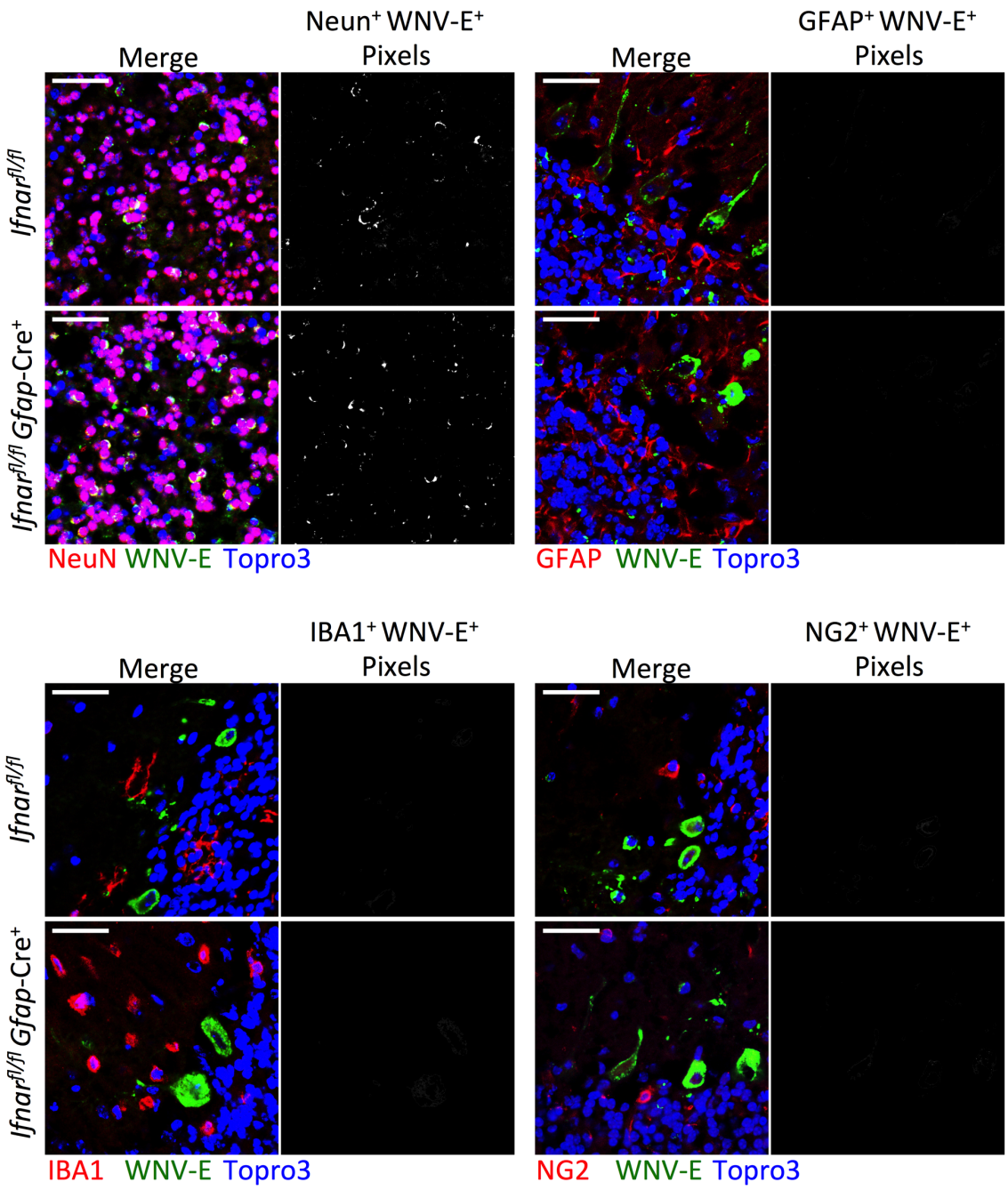

Figure S5: WNV-E protein staining localization in CNS following intracerebellar inoculation. Mice were infected via the intracerebellar route with 10 pfu WNV. Brains were removed on day 6 after infection and stained for WNV-E protein (green) and the neuronal marker NeuN, astrocyte marker GFAP, microglial marker IBA-1, or OPC marker NG2 (red). Nuclei in blue. Scale bar = 50 μm. Images are representative of at least 4 images taken for each of 5 independent mice per genotype.

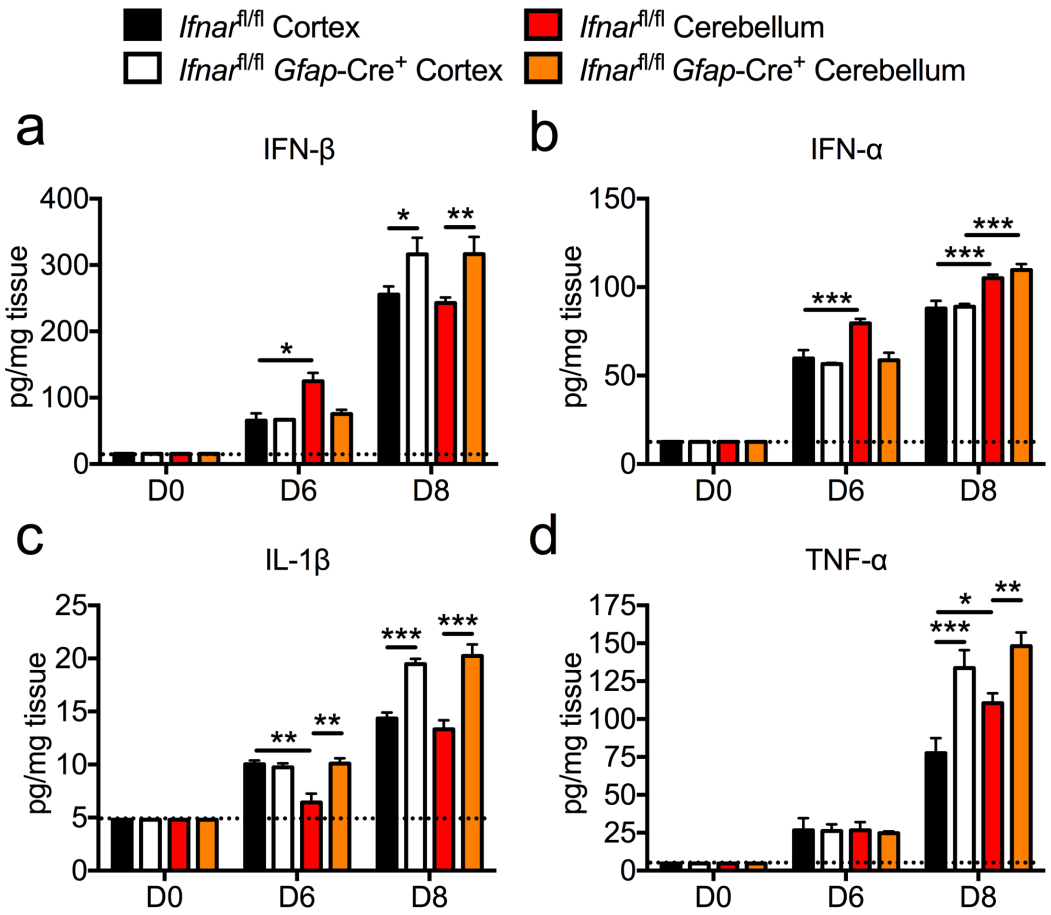

Figure S6: CNS cytokine expression following subcutaneous WNV infection. (a-d) ELISA analysis of indicated cytokine measured in homogenates of cerebral cortex or cerebellum harvested on day indicated following subcutaneous WNV infection. Data in **(a-d)** are mean values +/- SEM taken from 3 mice per genotype. All data were compared via two-way ANOVA.

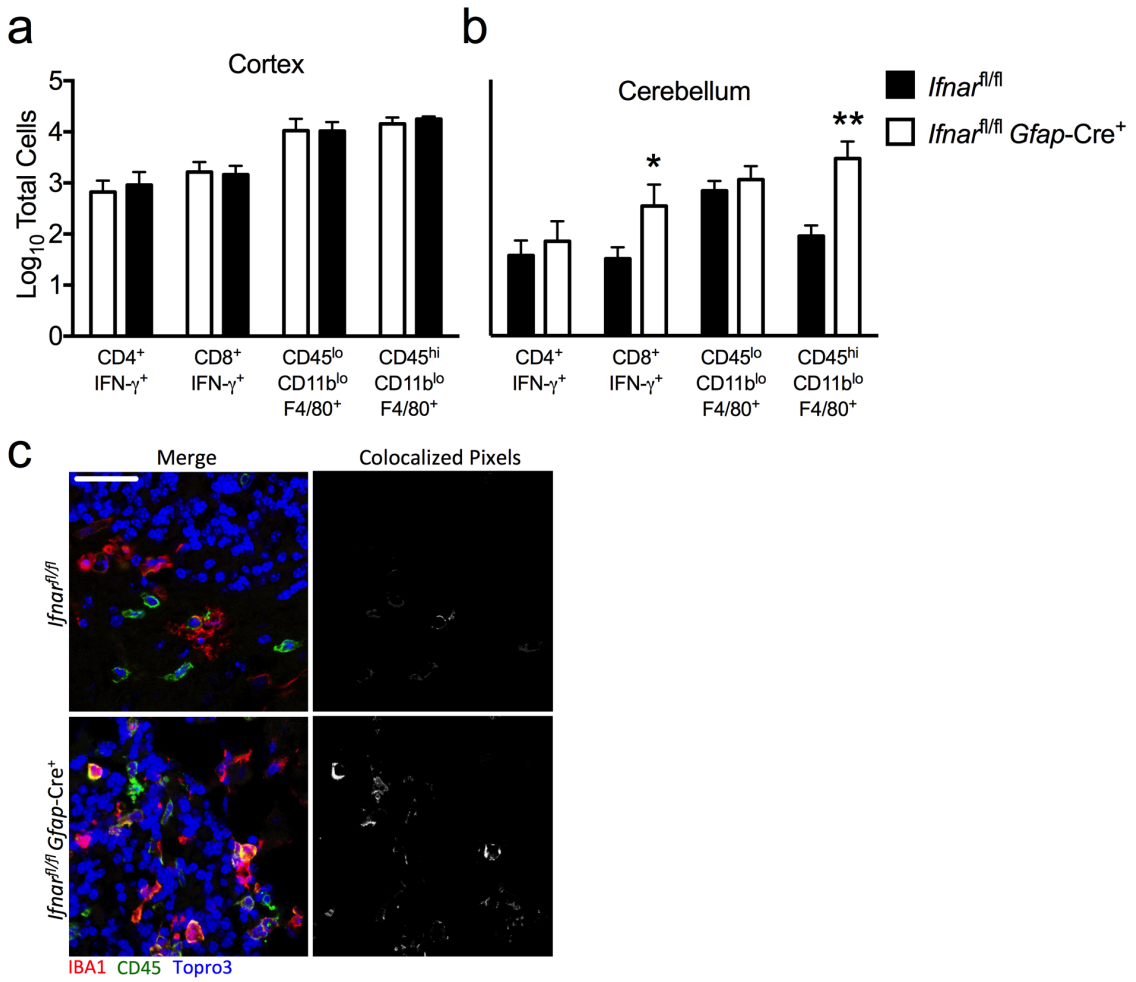

Figure S7: CNS immune cell trafficking following subcutaneous WNV infection. (**a-b**) Flow cytometric analysis of CNS immune cell infiltrates on day 8 following subcutaneous WNV infection. Values are total number of $CD45^{hi}$ $CD4^{+}$ and $CD45^{hi}$ $CD8^{+}$ lymphocytes expressing IFN-γ as well as $CD45^{lo}$ $CD11b^{+}$ (microglia) and $CD45^{hi}$ $CD11b^{+}$ (macrophages) isolated from (**a**) cortex or (**b**) cerebellum (after exclusion of doublets and dead cell debris). **(c)** IHC analysis of myeloid cells in cerebellar tissues of mice on D6 following intracerebellar inoculation with 10pfu WNV. Resident microglia are defined as $IBA1^{+}$ (red) $CD45^{neg\text{-}lo}$ (green), while infiltrating monocytes/macrophages are identified as $IBA1^{+}$ $CD45^{hi}$. Colocalized pixels are shown in the pixel masked images to the right of merged RGB images. Data in **(a-b)** are mean values +/- SEM taken from 6 mice collected from two independent experiments. All data were compared via unpaired, two-tailed student's t-test.

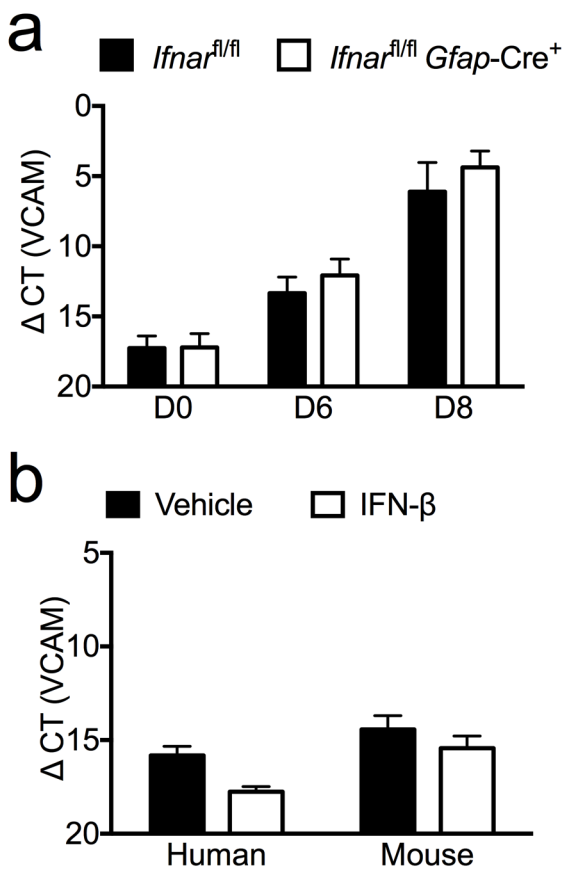

Figure S8: VCAM-1 expression in astrocytes *in vitro* and in the cerebral cortex *in vivo* following infection. (**a-b**) VCAM-1 mRNA levels were detected via SYBR qRT-PCR. (**a**) VCAM-1 mRNA levels were detected in the cerebral cortex of mice taken on indicated days following subcutaneous infection. Data for individual mice are normalized to expression of GAPDH. (**b**) VCAM-1 mRNA levels in primary adult human cerebral cortical astrocytes (left) or primary murine neonatal cerebral cortical astrocytes (right) following 4 h treatment with 10 U/ml of IFN-β. All data were compared via two-way ANOVA.

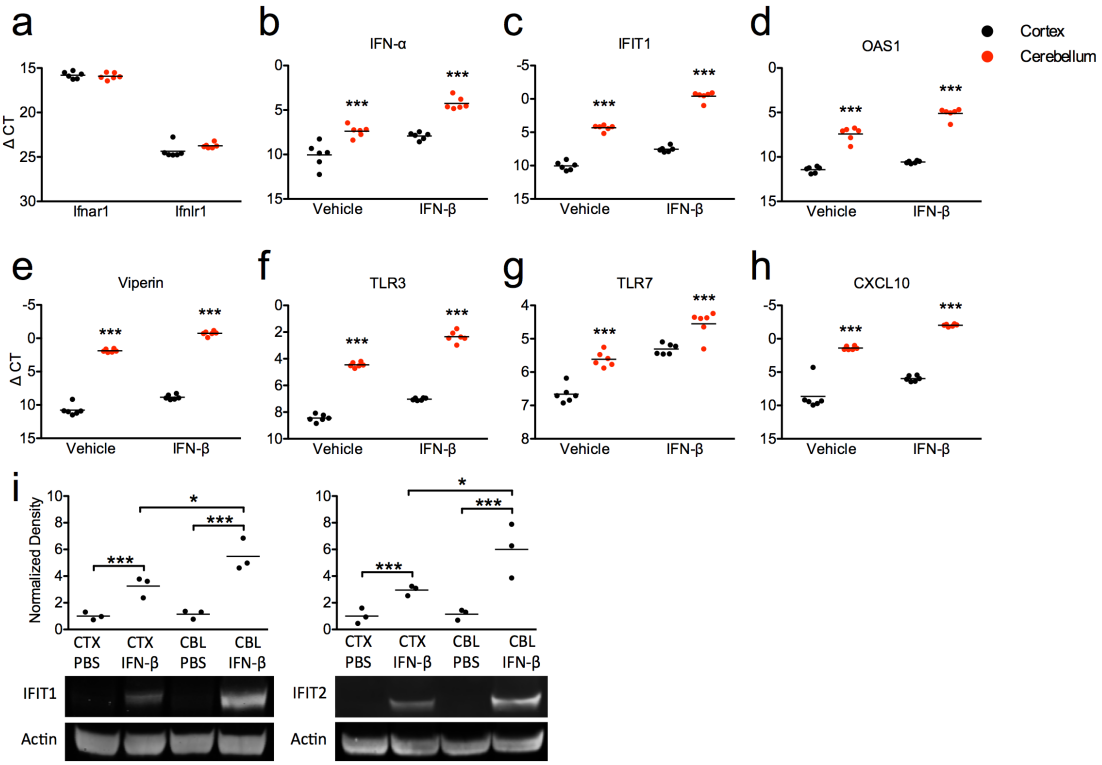

Figure S9: ISG expression in primary murine cerebral cortical and cerebellar astrocyte cultures. (**a**) Primary murine cerebral cortical or cerebellar astrocytes were assayed for basal expression of IFN receptors via Taqman qRT-PCR. Ct values are normalized to 18S ribosomal RNA (rRNA). (**b-h**) Astrocyte cultures were treated with 10 U/ml recombinant IFN-β or saline vehicle and analyzed for transcript expression of indicated genes at 4 hours post treatment via SYBR qRT-PCR. Ct values for all genes were normalized to Ct values of the housekeeping gene GAPDH. (**i**) Astrocyte cultures were treated as in (**b-h**) for 8 hours. Protein lysates were analyzed via western blot for expression of IFIT1 and IFIT2. Density values of individual samples are normalized to matched values for actin. Group means are normalized to mean values of PBS treated cortical astrocytes. Data in (**a-h**) represent 6 replicates taken from two independent experiments. Data in (**i**) are representative blots with quantification of three replicates derived from two independent experiments. All data were compared via two-way ANOVA.